

# Dosimetry in Peptide Radionuclide Receptor Therapy: A Review\*

Marta Cremonesi<sup>1</sup>, Mahila Ferrari<sup>1</sup>, Lisa Bodei<sup>2</sup>, Giampiero Tosi<sup>1</sup>, and Giovanni Paganelli<sup>2</sup>

<sup>1</sup>Division of Medical Physics, European Institute of Oncology, Milan, Italy; and <sup>2</sup>Division of Nuclear Medicine, European Institute of Oncology, Milan, Italy

The potential of targeted therapy with radiolabeled peptides has been reported in several clinical trials. Although there have been many improvements in dose estimation, a general and reliable dosimetric approach in peptide receptor radionuclide therapy (PRRT) is still a matter of debate. This article reviews the methods for PRRT dosimetry and the results presented in the literature. Radiopharmaceutical characteristics, data processing, dosimetric outcomes, and methods to protect critical organs are reported. The biological effective dose, based on the linear quadratic model, is also described.

**Key Words:** dosimetry; peptide receptor radionuclide therapy; <sup>111</sup>In; <sup>90</sup>Y; <sup>177</sup>Lu

**J Nucl Med 2006; 47:1467–1475**

**T**he utility of peptide receptor radionuclide therapy (PRRT) has been explored in clinical trials, and new radiopharmaceuticals are under development (1–7). Table 1 presents a list of radiopeptides in use in humans and other radioligands that are under investigation in preclinical studies. Kwekkeboom et al. (5) have recently shown quite encouraging results using a somatostatin analog (<sup>177</sup>Lu-DOTATATE [<sup>177</sup>Lu-DOTA<sup>0</sup>,Tyr<sup>3</sup>,Thr<sup>8</sup>]octreotide) in patients with neuroendocrine tumors. However, this and other phase I–II studies should be confirmed in large multicentric trials to establish the role of PRRT in clinical oncology. Moreover, a large field of technologic improvement must be developed to overcome some of the problems emerging from the pioneer studies. The high dose to kidney, bone marrow, and other nontarget tissues, as well as the large variability in biodistribution and tumor uptake among patients, should be addressed. Thus, precise and reliable

dosimetry of normal organs and tumor with these agents is needed, and its achievement is challenging.

Dose estimates to target organs are generally performed using the MIRD scheme (8). Cumulative activity in organs of interest can be determined by numeric or compartmental models (9) and absorbed dose calculations performed using dedicated software (OLINDA/EXM) (10,11). These programs have kinetic models and phantoms with reference parameters for patients of different size, age, and sex and also the possibility to include some patient-specific adjustments to the standard models. To improve the accuracy of activity to dose conversion, more sophisticated methods may include actual organ shape and size, inhomogeneous activity distributions, fused SPECT/CT images, and Monte Carlo codes (12). Once rough data are analyzed, the activities in normal tissues and tumor tissues must be converted into time–activity curves, and, finally, the absorbed doses must be estimated.

Somatostatin analogs are certainly the most clinically used radiopeptides, and this review will address mainly the results published for <sup>111</sup>In-DTPA-octreotide, <sup>90</sup>Y-DOTATOC, and <sup>177</sup>Lu-DOTATATE (Figs. 1A–1C).

## <sup>111</sup>IN-, <sup>90</sup>Y-, AND <sup>177</sup>LU-PEPTIDE DOSIMETRY

### <sup>111</sup>In-Peptides

The physical properties of <sup>111</sup>In make it suitable for both diagnostic and dosimetric purposes (Table 2). Dosimetry is facilitated by the  $\gamma$ -ray emission (173, 247 keV) and the relatively long half-life (2.83 d), which matches the peptide biologic half-life. Therefore, a suitable number of scintigraphic images can be obtained over >3 d (9,13) for dosimetry analysis. In principle, planar views are not ideal for dosimetry. However, serial whole-body scans might offer sufficient information on biodistribution and its variation over the time. This represents a good alternative to the more time-consuming SPECT technique, whose limited field of view usually requires 2 or more acquisitions for each time point.

<sup>111</sup>In-DTPA-octreotide is the commercially available <sup>111</sup>In-labeled compound used for diagnosis and staging of somatostatin receptor–positive tumors. <sup>111</sup>In-DOTATOC has

Received Feb. 6, 2006; revision accepted Jun. 12, 2006.

For correspondence or reprints contact: Giovanni Paganelli, MD, Divisions of Nuclear Medicine and Medical Physics, European Institute of Oncology, via Ripamonti, 435, 20141 Milan, Italy.

E-mail: direzione.mnu@ieo.it

\*NOTE: FOR CE CREDIT, YOU CAN ACCESS THIS ACTIVITY THROUGH THE SNM WEB SITE ([http://www.snm.org/ce\\_online](http://www.snm.org/ce_online)) THROUGH SEPTEMBER 2007.

COPYRIGHT © 2006 by the Society of Nuclear Medicine, Inc.

**TABLE 1**  
Radiopeptides for Targeted Radiotherapy

Peptide receptor	Radioligands used in humans for therapy	Radioligands in development
Somatostatin sst2	<sup>111</sup> In-DTPAOC <sup>90</sup> Y-DOTATOC <sup>177</sup> Lu-DOTATATE	Carbohydrated derivatives and other biodistribution modifiers
sst2, sst5 sst2, sst3, sst5	<sup>90</sup> Y-DOTA- <i>lanreotide</i>	DOTANOC DOTABOC DOTANOCate DOTABOCate TETA-octreotide
Bombesin GRP-R	<sup>177</sup> Lu-BNN8 analog	Bombesin analogs, including BBN8 analog, DOTA-[Lys <sup>3</sup> ]bombesin, and DOTA-PEG-BN(7–14)
Cholecystokinin CCK2		Minigastrin; CCK analog
Oxytocin		DOTALVT

DOTA = 1,4,7,10-tetraazacyclododecane-1,4,7,10-tetraacetic acid; DTPA = diethylenepentaacetic acid; <sup>111</sup>In-DTPAOC = [<sup>111</sup>In-DTPA<sup>0</sup>,<sub>D</sub>-Phe<sup>1</sup>]octreotide; <sup>90</sup>Y-DOTATOC = [<sup>90</sup>Y-DOTA,Tyr<sup>3</sup>]octreotide; <sup>90</sup>Y-DOTA-*lanreotide* = [<sup>90</sup>Y-DOTA,Tyr<sup>3</sup>]lanreotide; <sup>177</sup>Lu-DOTATATE = [<sup>177</sup>Lu-DOTA<sup>0</sup>,Tyr<sup>3</sup>,Thr<sup>8</sup>]octreotide; DOTANOC = [DOTA,1-Nal<sup>3</sup>]octreotide; DOTABOC = [DOTA,BzThi<sup>3</sup>]octreotide; DOTANOCate = [DOTA,1-Nal<sup>3</sup>,Thr<sup>8</sup>]octreotide; DOTABOCate = [DOTA,BzThi<sup>3</sup>,Thr<sup>8</sup>]octreotide; TETA-octreotide = 1,4,8,11-tetraazacyclotetradecane-*N,N',N'',N'''*-tetraacetic acid-octreotide; <sup>177</sup>Lu-BNN8 analog = <sup>177</sup>Lu-DO3A-CH<sub>2</sub>CO-G-4-aminobenzoyl-Q-W-A-V-G-H-L-M-NH<sub>2</sub>; DOTA-[Lys<sup>3</sup>]bombesin = [DOTA-Lys<sup>3</sup>]bombesin; DOTA-PEG-BN(7–14) = [DOTA-PEG]bombesin; CCK2 = cholecystokinin dipeptide; DOTALVT = [DOTA,Lys<sup>8</sup>]vasotocin.  
Modified from Reubi et al. (7).

been also used in clinical protocols (14–17) for dosimetric analysis when planning therapy.

The idea of using <sup>111</sup>In-coupled peptides for therapy—in particular, <sup>111</sup>In-DTPA-octreotide (18,19)—stems from the possible benefit of the Auger emission of this radionuclide. Auger electrons are high linear energy transfer particles, able to deliver high doses within a very short range (<10 μm). However, the high cytotoxic potential of the Auger electrons requires close proximity of the <sup>111</sup>In-labeled peptide within the nucleus, preferably intercalating with the DNA chain (20).

The pharmacokinetics of <sup>111</sup>In-DTPA-octreotide demonstrate fast blood clearance, with low exposure of the whole body (13,19). Activity is excreted through the kidneys, with a very small activity in the bowel (<2%). No specific uptake of the tracer is usually observed in bone marrow, allowing the blood-derived method to be used for dose evaluation (0.01–0.06 mGy/MBq). The organs receiving the highest dose (Fig. 1A) are the spleen (0.10–0.85 mGy/MBq), the kidneys (0.12–0.91 mGy/MBq), and the liver (0.05–0.24 mGy/MBq). The absorbed dose to tumor, evaluated as the mean energy released to the whole tumor tissue, varies widely (0.7–30.5 mGy/MBq).

Despite some encouraging preliminary results, clinical trials with <sup>111</sup>In-DTPA-octreotide showed only rare cases of tumor regression (4). This probably relates to the limited effect of Auger energy, likely because the nuclide is probably too far from the nucleus.

#### <sup>90</sup>Y-Peptides

<sup>90</sup>Y is a high-energy β<sup>-</sup>-emitter (E<sub>ave, β</sub> = 0.935 MeV), with a physical half-life (T<sub>1/2 phys</sub> = 64.1 h) compatible with the pharmacokinetics of peptides, and a long penetration range in tissue (R<sub>max</sub> = 11.3 mm). Thus, <sup>90</sup>Y is particularly suitable for radionuclide therapy, considering the nonhomogeneous distribution of peptides in solid tumors (Table 2). The probability of killing most neoplastic cells is related to the so-called cross-fire effect. However, there is a relatively high radiation exposure to normal tissues, such as liver, kidneys, and spleen.

<sup>90</sup>Y-DOTATOC, <sup>90</sup>Y-DOTATATE, and <sup>90</sup>Y-*lanreotide* are the principal <sup>90</sup>Y-labeled radiopharmaceuticals used for PRRT therapy (4,6,21). A major drawback of <sup>90</sup>Y-labeled peptides is the lack of γ-emission, which makes it difficult to get specific dosimetry in each patient. To estimate a specific dose, alternative methods such as imaging with analogs labeled with <sup>111</sup>In or substituting the positron emitter <sup>86</sup>Y for <sup>90</sup>Y may be used (15,16,22–24).

**<sup>111</sup>In-Based Methods.** The first approach simulated therapy with <sup>90</sup>Y-compounds using diagnostic activities of <sup>111</sup>In-DTPA-octreotide (14,24). <sup>111</sup>In-DTPA-octreotide is limited as a surrogate for <sup>90</sup>Y-DOTATOC because of the difference in chelators and the single amino acid modification of the octreotide (24). A more suitable alternative uses the same peptide as the therapeutic agent labeled with <sup>111</sup>In. If the biologic behavior of the <sup>90</sup>Y and <sup>111</sup>In analogs is similar *in vivo*, this approach is useful (6,15,17). Images derived from

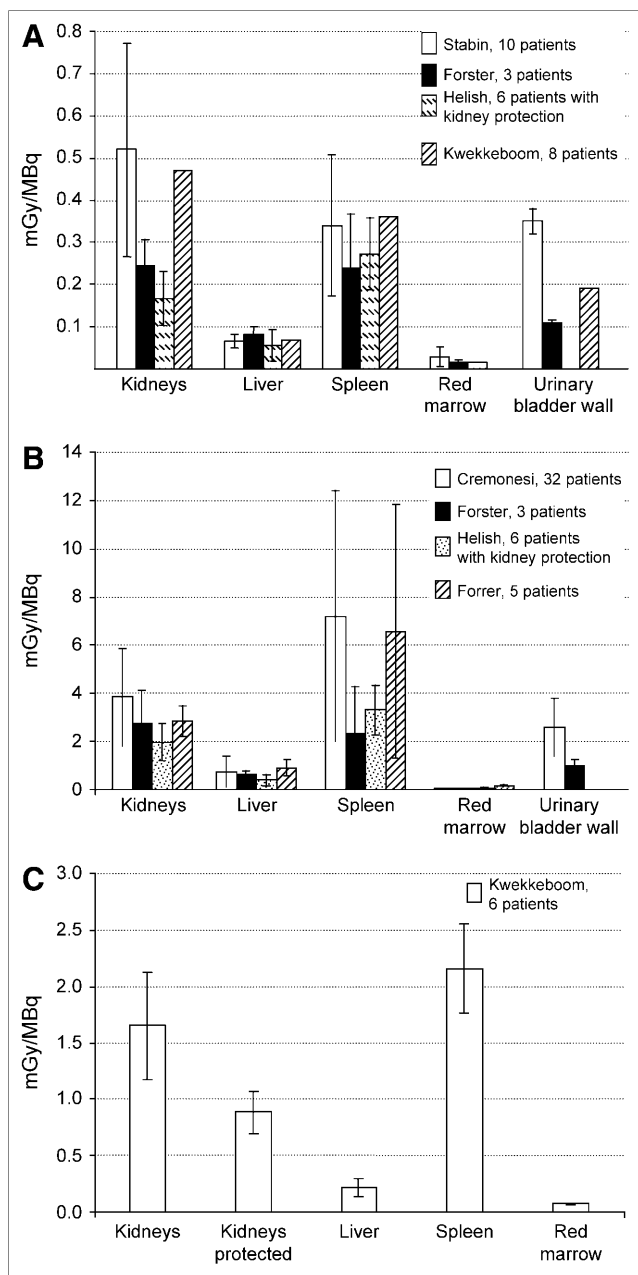


**FIGURE 1.** Dosimetric data published for principal PRRT trials: (A) <sup>111</sup>In-DTPA-octreotide (Stabin (13), Forster (22), Helish (23), Kwekkeboom (14)). (B) <sup>90</sup>Y-DOTATOC (Cremonesi (15), Forster (22), Helish (23), Forrer (16)). (C) <sup>177</sup>Lu-DOTATATE (Kwekkeboom (30)). Large ranges of variability emerge, even in large cohort of patients. This suggests that mean values of absorbed doses among patients should not be the only criterion to plan PRRT. Besides the methods used for dosimetry, interindividual differences are attributable, especially to organ functionality, metabolism, or receptor density in organs.

<sup>111</sup>In-DOTATOC, <sup>111</sup>In-DOTATATE, and <sup>111</sup>In-lanreotide visibly reflect the higher in vivo affinity and specific uptake in somatostatin receptor-expressing tissues, and especially in the tumor, compared with <sup>111</sup>In-DTPA-octreotide (5,6,14,24). To date, imaging and pharmacokinetics analysis with <sup>111</sup>In-labeled peptides remain a feasible and reliable

procedure (17,24). Moreover, the most relevant advantage of this approach is in the physical half-life of <sup>111</sup>In, comparable with that of <sup>90</sup>Y and with the biologic half-life of peptides, which allows derivation of the time-activity curves.

**<sup>86</sup>Y-Based Methods.** Although the chemical behavior of <sup>111</sup>In-DOTATOC is similar to that of the analog labeled with <sup>90</sup>Y, the chemical nature of the radionuclide may affect the binding affinity for somatostatin receptors (25). To address this question, the labeling of the same compound with the positron emitter of the same element <sup>86</sup>Y has been introduced. In particular, the biokinetics of <sup>86</sup>Y-DOTATOC, totally preserving the chemical structure of <sup>90</sup>Y-DOTATOC, has been investigated and is generally considered as the gold standard for mimicking therapy. Although a comparison of <sup>111</sup>In-DOTATOC versus <sup>86</sup>Y-DOTATOC, in the same patients, is desirable, the biokinetics of <sup>111</sup>In-DTPA-octreotide versus <sup>86</sup>Y-DOTATOC have been compared instead. The results indicated that although <sup>111</sup>In-DTPA-octreotide is not the optimal surrogate for measuring dosimetry for <sup>90</sup>Y-DOTATOC, it may yield acceptable results for certain clinical applications—in particular, for patient recruitment in clinical trials (22–24).

PET has the advantage of increased accuracy and spatial resolution (21). Nevertheless, the use of <sup>86</sup>Y for PRRT dosimetry is presently limited by the availability of <sup>86</sup>Y. In addition, the  $T_{1/2 \text{ phys}}$  of 14.7 h and the positron abundance of 33% limit the detailed data acquisition to <40 h (Table 2). Late activity concentrations are not experimentally obtainable and must be estimated by extrapolation, reducing the reliability of the integrated activities. This is especially true for tissues with a delayed clearance or metabolism, such as the kidneys. Additional technical problems occur because of the emission of multiple, high-energy,  $\gamma$ -rays in a cascade in the course of decay of <sup>86</sup>Y (26). Extrapolation of the <sup>86</sup>Y distribution to <sup>90</sup>Y dosimetry requires correction for these factors, as proposed by several authors (27,28). Inadequate corrections may lead to important activity overestimations, especially in bone and bone marrow.

A summary of the dosimetric results of <sup>90</sup>Y-DOTATOC using both <sup>111</sup>In-DOTATOC and <sup>86</sup>Y-DOTATOC is shown in Figure 1B. Besides the method selected, results were concordant on some essential aspects: (a) the pharmacokinetics data of <sup>90</sup>Y-DOTATOC showed a very fast blood clearance and rapid urinary elimination; (b) the highest predicted absorbed doses were found in the spleen (range, 1.5–19.4 mGy/MBq), kidneys (range, 1.06–10.3 mGy/MBq), and liver (range, 0.1–2.6 mGy/MBq). As for the absorbed dose to the red marrow, most authors did not report any significant uptake in bone or bone marrow and used blood-derived methods. The dose values ranged from 0.01 to 0.20 mGy/MBq and from 0.04 to 0.08 mGy/MBq when evaluated by <sup>111</sup>In-DOTATOC or <sup>86</sup>Y-DOTATOC, respectively. Other authors observed some uptake in the red marrow by <sup>86</sup>Y-DOTATOC images (29). Higher red marrow doses (0.11–0.23 mGy/MBq) were reported in this case, although the information provided by <sup>86</sup>Y-images remains uncertain.

**TABLE 2**  
Characteristics of Radionuclides for PRRT

Radionuclide	T <sub>1/2 phys</sub>	Useful emission	Energy	Particle range in tissue	Application
Principal radionuclides used in clinical trials for PRRT					
<sup>111</sup> In	67.4 h	γ e <sup>-</sup> Auger e <sup>-</sup> IC	Eγ: 173 (87%), 247 (94%) keV E: 0.5–25 keV E: 144–245 keV	R <sub>max</sub> : 0.02–10 μm R <sub>max</sub> : 200–550 μm	Imaging, therapy
<sup>90</sup> Y	64.1 h	β <sup>-</sup>	E <sub>max, β<sup>-</sup></sub> : 2.28 MeV E <sub>ave, β<sup>-</sup></sub> : 935 keV	R <sub>max</sub> : 11.3 mm R <sub>mean</sub> : 4.1 mm	Therapy
<sup>177</sup> Lu	6.73 d	β <sup>-</sup> γ	E <sub>max, β<sup>-</sup></sub> : 497 keV E <sub>ave, β<sup>-</sup></sub> : 149 keV Eγ: 113 (6%), 208 (11%) keV	R <sub>max</sub> : 2 mm R <sub>mean</sub> : 0.5 mm	Imaging, therapy
Principal radionuclides used in clinical trials for imaging					
<sup>86</sup> Y	14.7 h	β <sup>+</sup>	E <sub>max, β<sup>+</sup></sub> : 1.22 (13%), 1.55 (6%), 2.0 (4%) MeV E <sub>ave, β<sup>+</sup></sub> : 660 keV Eγ: 0.443 (17%), 0.628 (33%), 1.08 (83%), 1.15 (31%), 1.92 (21%) MeV		Imaging
<sup>68</sup> Ga	68 min	β <sup>+</sup>	E <sub>max, β<sup>+</sup></sub> : 1.90 (89%) MeV E <sub>ave, β<sup>+</sup></sub> : 830 keV	R <sub>max</sub> : 9 mm R <sub>mean</sub> : 1 mm	Imaging
Other radionuclides under investigation for potential applications					
<sup>18</sup> F	1.83 h		E <sub>max, β<sup>+</sup></sub> : 634 (97%) keV E <sub>mean, β<sup>+</sup></sub> : 250 keV	R <sub>max</sub> : 2.4 mm R <sub>mean</sub> : 0.6 mm	Imaging
<sup>64</sup> Cu	12.8 h	β <sup>-</sup> β <sup>+</sup>	E <sub>max, β<sup>-</sup></sub> : 570 (37%) keV E <sub>max, β<sup>+</sup></sub> : 653 (18%) keV E <sub>mean, β<sup>+</sup></sub> : 278 keV	R <sub>max</sub> : 2.5 mm R <sub>mean</sub> : 0.7 mm	Imaging, therapy
<sup>67</sup> Cu	61 h	β γ	E <sub>max, β<sup>-</sup></sub> : 40 (57%), 480 (22%), 580 (20%) keV Eγ: 90–93 (24%), 182 (44%) keV	R <sub>max</sub> : 0.4 mm R <sub>mean</sub> : 0.2 mm	Imaging, therapy
<sup>166</sup> Ho	26.8 h	β	E <sub>max, β<sup>-</sup></sub> : 1.85 MeV E <sub>mean, β<sup>-</sup></sub> : 711 keV Eγ: 81 (7%) keV	R <sub>max</sub> : 8.7 mm R <sub>mean</sub> : 0.9 mm	Imaging, therapy
<sup>188</sup> Re	17.0 h	β <sup>-</sup>	E <sub>max, β<sup>-</sup></sub> : 1.96 (20%), 2.12 (78%) MeV E <sub>mean, β<sup>-</sup></sub> : 765 keV Eγ: 155 (10%) keV	R <sub>max</sub> : 11 mm R <sub>mean</sub> : 3.8 mm	Imaging, therapy

IC = internal conversion; R<sub>max</sub> = range in tissue after which 95% of particles are stopped; R<sub>mean</sub> = mean range in tissue; T<sub>1/2 phys</sub> = physical half-life; E<sub>max</sub> = maximum β-particle energy per disintegration; E<sub>ave</sub> = average β-particle energy per disintegration.

Diagnostic studies demonstrated highly variable tumor doses with both <sup>111</sup>In-DOTATOC and <sup>86</sup>Y-DOTATOC (15, 16,23) (Table 3). Nonetheless, the efficacy of PRRT with <sup>90</sup>Y-DOTATOC has been observed in several clinical trials. The major drawback of <sup>90</sup>Y-peptides is that the activity administered is limited by the high renal dose, which can preclude the achievement of a prescribed tumor dose.

#### <sup>177</sup>Lu-Peptides

The physical properties of <sup>177</sup>Lu offer intermediate advantages between <sup>90</sup>Y and <sup>111</sup>In (Table 2). <sup>177</sup>Lu is a β<sup>-</sup>-particle emitter (E<sub>max</sub> = 0.50 MeV), with a long half-life (6.73 d), and a R<sub>50</sub> (the distance within which the β-particles of <sup>90</sup>Y transfer 50% of their energy) of approximately 1 mm. It is also a γ-emitter of low-emission abundance (113 [6%] and 208 [11%] keV). These characteristics enable imaging and therapy with the same complex and allow dosimetry to be performed before and during treatment as well. Comparison of its penetration range in tissue (R<sub>max</sub> = 2 mm) with <sup>90</sup>Y indicates a lower cross-fire effect partially compensated by a higher percentage of the radiation energy absorbed in very small volumes. This makes <sup>177</sup>Lu a good candidate nuclide for the treatment of small tumors (<2 cm) and micrometastases with <sup>177</sup>Lu-DOTATATE.

A study comparing <sup>177</sup>Lu-DOTATATE with <sup>111</sup>In-DTPA-octreotide (30) demonstrated similar biologic half-lives and principal source organs for the 2 radiocompounds, with varying uptakes in organs and lesions with different expression of somatostatin receptors. These results support the use of similar methods for data collection and similar time schedules for the dosimetry of both <sup>111</sup>In-peptides and <sup>177</sup>Lu-peptides, although experimental data for the time-activity curves can be further prolonged in the latter case.

The dosimetric data on <sup>177</sup>Lu-DOTATATE (Fig. 1C) are still limited (4,5,30). The blood clearance and urinary excretion are fast, similar to the other somatostatin analogs described. The dosimetry of normal organs is lower for <sup>177</sup>Lu-DOTATATE as compared with <sup>90</sup>Y-DOTATOC, with ranges of 1.8–2.7 mGy/MBq to the spleen, 1.0–2.2 mGy/MBq to the kidneys (lowered to 0.7–1.1 mGy/MBq with protection), and 0.1–0.3 mGy/MBq to the liver. Red marrow dose, derived by the blood approach, ranged from 0.05 to 0.08 mGy/MBq (30). Although the absorbed dose to the gonads has not been reported in the literature, a significant decrease of serum testosterone has been observed, which requires 18–24 mo for reversal (5). This

**TABLE 3**  
Tumor Dosimetry for Principal Radiopharmaceuticals Used in PRRT

Radiopharmaceutical	Tumor mass (g)	Absorbed dose (mGy/MBq)	Reference
<sup>111</sup> In-DTPA-octreotide	1 g*	6.9	(30)
	10 g*	0.7	(30)
		2.8, for RBE = 1	(18)
		11.2, for RBE = 20	(18)
	100 g*	0.4, for RBE = 1	(18)
	1.3, for RBE = 20	(18)	
<sup>90</sup> Y-DOTATOC	9 lesions (mass not specified)	Range = 2.4–41.7 <sup>†</sup>	(16)
	23 lesions; range = 2–115 g	Range = 1.4–31.0 <sup>†</sup>	(15)
	Mass not specified	Range = 2.1–29.5 <sup>‡</sup>	(23)
<sup>177</sup> Lu-DOTATATE	1 g*	37.9	(30)
	10 g*	3.9	(30)

\*Tumor masses considered for theoretic tumor dose evaluations.

<sup>†</sup><sup>111</sup>In-DOTATOC used as radiotracer.

<sup>‡</sup><sup>86</sup>Y-DOTATOC used as radiotracer.

RBE = relative biologic effectiveness; <sup>111</sup>In-DTPA-octreotide = [<sup>111</sup>In-DTPA<sup>0</sup>,D-Phe<sup>1</sup>]octreotide; <sup>90</sup>Y-DOTATOC = [<sup>90</sup>Y-DOTA,Tyr<sup>3</sup>]octreotide; <sup>177</sup>Lu-DOTATATE = [<sup>177</sup>Lu-DOTA<sup>0</sup>,Tyr<sup>3</sup>,Thr<sup>8</sup>]octreotide.

effect is likely secondary to the high activity received by the urinary bladder, with consequent irradiation of the gonads from  $\gamma$ -rays, especially in men, or even to a possible local uptake.

### Tumor Dosimetry

A high variability of inpatient and intralesion tumor uptake has been seen in PRRT studies, which is independent of the radiopharmaceuticals used (Table 3). The wide range of tumor doses was not surprising, likely related to biologic and pathologic factors—differences in tumor volume, hypoxia, necrosis, viability, interstitial pressure, heterogeneity in binding affinity, and the receptor density.

Interestingly, a correlation between tumor dose and tumor mass reduction has been reported (24). Responding tumors could be identified as those receiving much higher doses compared with nonresponding tumors (up to 6-fold: 232 Gy vs. 37 Gy). This emphasized the challenge to deliver the highest activity to the tumor, while sparing normal tissues.

The most suitable choice of the radiopharmaceutical is crucial in therapy planning and should be performed individually, based on tumor volume and localization, adjacent tissues, and affinity for the targeting compound. As peptides are internalized, the physical characteristics of the radionuclide should be fully exploited. The lower tissue penetration range of <sup>177</sup>Lu may reasonably exert a more favorable effect on small tumors compared with <sup>90</sup>Y. Conversely, the cross-fire effect of <sup>90</sup>Y may induce a superior radiation burden in larger lesions. New perspectives pursue the use of cocktails of <sup>177</sup>Lu- and <sup>90</sup>Y-radiopeptides, promising the treatment of different-sized lesions. Preclinical animal studies showed encouraging data, and the radiobiologic value of these cocktails will hopefully be addressed in patients in the very near future (31).

### Red Marrow Dosimetry

Red marrow toxicity represents the limiting factor in numerous radionuclide therapies. Several investigators describe models for red marrow dosimetry and tolerance (10,32). Nevertheless, red marrow has a very complex structure, and the mechanisms regulating activity uptake are still not clear. Marrow radiation burden varies with the radio-labeled molecule, the specific binding, and the residual activity in the blood. Difficulties in modeling the dosimetry of red marrow are therefore comprehensible and are well illustrated in the literature (11,33,34).

The principal approaches used to evaluate the red marrow dose can be distinguished in blood-based methods and imaging-based methods.

The blood-based method was expressly investigated in the study of radiolabeled monoclonal antibodies (mAbs) in cases of no specific uptake in the red marrow (35). The activity concentration in the red marrow was linearly related to the activity concentration in the blood or in the plasma by an experimental factor (in the range of 0.2–0.4, for mAbs, likely related to their molecular weight). The possibility of implementing the blood-based method in PRRT needs an additional parameter, as peptide-bound activity in the red marrow probably distributes in a volume larger than the extracellular space. Moreover, few bone marrow samples taken in patients receiving <sup>111</sup>In-DTPA-octreotide showed a red marrow activity concentration equal to that in plasma at the same time points (36,37). Consequently, for peptides, a factor for the concentration ratio of red marrow to blood close to 1 has been suggested.

The image-based method applies when images clearly demonstrate a specific uptake in bone or bone marrow. In this case, the activity in selected areas of known red marrow volume (e.g., sacrum, lumbar vertebrae) is quantified from images and scaled for the whole red marrow. In most

studies with somatostatin analogs, no specific bone marrow localization is seen, and the blood activity is used as a surrogate indicator. Images of  $^{111}\text{In}$ - or  $^{177}\text{Lu}$ -labeled somatostatin analogs usually do not evidence any significant uptake in red marrow or in bone. Consequently, many authors prefer to extrapolate the red marrow dose from the time-activity curve in the blood, plasma, or remainder of the body (15,22). Assessment of bone marrow dose in most radionuclide therapies remains a challenge (32–34).

### Other Radiopeptides of Interest for PRRT

Besides the radiopeptides already in use for therapeutic purposes, other radiocompounds are worth mentioning for their potential role in PRRT (Table 1). Among these, the development of peptides labeled with positron-emitter radionuclides is of special interest. In particular,  $^{68}\text{Ga}$  is a very attractive  $\beta^+$ -emitter radionuclide because of its availability from a generator. Somatostatin and bombesin derivatives labeled with  $^{68}\text{Ga}$  have shown ideal characteristics, such as fast clearance and target localization in clinical studies. Recently,  $^{68}\text{Ga}$ -DOTATOC has been shown to provide excellent diagnostic information in patients. Although its biokinetics may not be ideal to mirror the dosimetry of therapeutic agents, it may have a main role in the prediction of the PRRT response and follow-up (38,39).

Other radiopeptides investigated in preclinical studies have given valuable results, not only for imaging, such as [ $^{18}\text{F}$ ]FP-Gluc-TOCA (40) but also for therapy, including bombesin derivatives labeled with  $^{166}\text{Ho}$  and  $^{188}\text{Re}$  (7), and bombesin and somatostatin derivatives labeled with  $^{64}\text{Cu}$  and  $^{67}\text{Cu}$  ( $^{64}\text{Cu}$ -DOTA-[Lys $^3$ ]bombesin (41),  $^{64}\text{Cu}$ -DOTA-PEG-BN(7–14) (42),  $^{64}\text{Cu}$ -TETA-octreotide (43)).  $^{64}\text{Cu}$ -TETA-octreotide, administered in a small number of patients with neuroendocrine tumors, showed clear lesion detection and had favorable pharmacokinetics (43). The special attention merited by Cu-labeled peptides is related to the physical characteristics of  $^{67}\text{Cu}$  and of  $^{64}\text{Cu}$ , which are especially suitable for both imaging and therapy ( $^{67}\text{Cu}$ ,  $\gamma$ -imaging/PRRT;  $^{64}\text{Cu}$ , PET imaging/PRRT).

### KIDNEY DOSIMETRY: METHODS, PITFALLS, AND IMPROVEMENTS

All the radiopharmaceuticals used for PRRT have shown high renal activity concentration. This has shifted—or enlarged—the general concern of toxicity from red marrow to kidneys. Kidneys are dose-limiting organs for PRRT—in particular, with  $^{90}\text{Y}$ -DOTATOC (3,24,44)—making accurate renal dosimetry critical to minimize radiation nephropathy.

In most cases side effects were unforeseen or were not correlated with the administered activity or with the calculated kidney dose. In other cases, such as in therapy with  $^{111}\text{In}$ -DTPA-octreotide or  $^{177}\text{Lu}$ -DOTATATE, despite the high kidney doses (comparable with those using  $^{90}\text{Y}$ -peptide therapies), alteration of renal function parameters was much lower than expected. These findings were surprising, as the

occurrence of nephritis was believed to be determined, in principle, by radiation dose. The alarming high doses to kidneys, and—most importantly—cases of late renal failure in patients who received kidney doses below the conventional threshold dose derived from external-beam radiotherapy (EBRT) (44,45) suggested the need to reexamine this problem.

The first evaluations of kidney dosimetry were usually based on a robust standard approach, assuming uniform activity distributions and standard masses within the MIRD scheme. However, the excessive interpatient variability of kidney absorbed doses suggested the need for more precise measurements. A first crucial improvement in renal dosimetry was obtained by the inclusion of the actual kidney masses (derived from CT) in the dosimetric estimates. Patient kidney volumes varied between 231 and 503 mL (in 25 patients), some values being very far from the reference volumes of 288 mL (male) and 264 mL (female). Consequently, kidney absorbed doses rescaled by the true masses provided values differing up to 100%. The relevance of this simple correction has been recently confirmed in a retrospective clinical study, in which the unexpected renal toxicity in a few patients could be explained by the significantly smaller kidney mass (24).

A further contribution to inaccuracy occurred because of the nonuniform radioactivity distribution in the kidney. Scintigraphic images demonstrated higher and persistent uptake in the cortex compared with the medulla. Unfortunately, the spatial resolution of SPECT or PET/CT equipment, can indicate—but not precisely establish—the fine differences among subregions. This has been confirmed by ex vivo autoradiography in patients receiving  $^{111}\text{In}$ -DTPA-octreotide (46). These experimental findings could open the way to more accurate renal dosimetry.

To face the problem of uneven uptake in the kidney, the MIRD Committee offered a multiregion model for a suborgan kidney dosimetry (10,47)—with cortex, medulla, pelvis, and papillae as possible source or target regions. In particular, in patients undergoing PRRT, specific kidney dose evaluations can be obtained by rescaling the actual volumes of the renal regions and by the activity assigned to cortex and medulla, evaluated, for example, by PET or SPECT images or, more accurately, by voxel-based methods (48–50). Alternatively, the experimental results of renal autoradiograms can be considered as rational for detailed kidney dosimetry (50).

In addition to the suborgan activity distribution, the physical characteristics of the radionuclide can be a major determinant of the nephrotoxic potential of the agent and, hence, of the risk–benefit balance. This has been confirmed clinically by the frequent occurrence of renal impairment in patients treated with  $^{90}\text{Y}$ -peptide therapy compared with the sporadic incidence observed with  $^{111}\text{In}$ -DTPA-octreotide and  $^{177}\text{Lu}$ -TATE therapies (despite mean cumulative kidney doses up to 45 Gy) (3,51). Two potential explanations are the particle range and the site of peptide accumulation: localization in the proximal tubuli, with their radioresistant

cells, able to repair and regenerate, versus the glomeruli with their radiosensitive cells, not able to regenerate, can make a major difference in outcome. Therefore, the Auger electrons of  $^{111}\text{In}$ -peptides, and also the short-range  $\beta$ -particles of  $^{177}\text{Lu}$ -peptides, irradiate the tubular cells more selectively compared with the glomeruli. On the contrary, the long-range  $\beta$ -particles of  $^{90}\text{Y}$ -peptides may increase the toxicity due to the irradiation of the glomerular cells.

### Methods for Possible Kidney Dose Reduction

It has been observed that renal uptake is not somatostatin receptor driven but related primarily to the very rapid clearance of the small radiopeptides that are filtered through the glomeruli and reabsorbed by the tubular cells (24,25,52). Preclinical and clinical studies showed that the infusion of positively charged amino acids (e.g., lysine, arginine)—before, during, and after the injection of the radioligand—is able to block the tubular peptide reabsorption process (2,25,51,53). On the basis of these findings, the efficacy and side effects of several renal protector regimens were tested. Different amounts of amino acid solutions and combinations with other positively charged molecules were studied, and the timing, the duration of the infusion, and the amino acid toxicity (mostly gastrointestinal) were analyzed (2,50,51,54–57).

The results of  $^{86}\text{Y}$ -DOTATOC or  $^{111}\text{In}$ -DOTATOC as a radiotracer to determine tracer retention in the kidneys after pretreatment with amino acids can be summarized as follows:

- (a) The blood clearance and the activity elimination are not substantially modified by renal protectors; tumor uptake is not altered; and the biodistribution in source organs other than kidneys leads to minimal changes (mostly in the spleen).
- (b) Protector agents maintain the typical trend of the time–activity curves in kidneys but reduce the renal uptake at all time points; and absorbed doses are consistently lowered 20%–30% (up to 40%) by amino acids or 30%–40% (up to 55%) by other positively charged molecule combinations.
- (c) Both the total dose and the duration of the infusion influence the dose sparing (up to 65%, with a combination of positively charged molecules infused over 2 d after injection).

### Dose and Dose Rate: Linear Quadratic (LQ) Model from EBRT to PRRT

According to the experience gained from EBRT, absorbed doses to the kidneys of 23 and 28 Gy are associated with a 5% ( $\text{TD}_{5/5}$  [dose for a probability of 5% injury within 5 y]) probability and a 50% ( $\text{TD}_{50/5}$  [dose for a probability of 50% injury within 5 y]) probability of causing deterministic late side effects within 5 y, respectively. It is also known that doses of >25 Gy may lead to acute radiation nephropathy with a latent period of 6–12 mo, whereas, at lower doses, chronic radiation nephropathy

may become clinically apparent 1–5 y after irradiation (58). Unfortunately, these findings do not apply to internal radionuclide therapies. Although the general radiobiologic principles are the same, the radiation dose delivered during radionuclide therapy differs in many respects from a dose delivered by EBRT. First, the radiation dose rate in EBRT is high (1–3 Gy/min) and the total prescribed dose is delivered in some fractions (typically, 2 Gy/fraction); in contrast, the radiation dose rate in PRRT is low (<3 mGy/min) and variable, with a continuous exponential decrease related to biologic and physical decay (59,60).

The dose rate has a most important radiobiologic impact, in that it may alter the recovery from radiation damage. This has been widely investigated and demonstrated in EBRT, and it is well known that, at equal dose, fractionation of EBRT lowers toxicity. In general, early-responding tissues (most tumors) are characterized by cell-survival curves with smaller shoulders compared with late-responding tissues (60). The influence of the dose rate may be even more relevant in radionuclide therapy compared with EBRT, as the variability of both dose rate and dose distribution might strengthen the reparable sublethal damage: the lower the dose rate, the lower the damage (61). These considerations suggest that the sparing effect should benefit the tumor-to-kidney dose ratio in PRRT, as the kidney is a late-responding tissue.

Recently, some authors have used the LQ model to quantify the dose-rate sparing concepts expressly for radionuclide therapy, taking into account the different dose rate as compared with EBRT (61). The LQ model describes the biologic effect in irradiated tissue by the surviving fraction (S) of cells that received a radiation dose D:

$$S = \exp(-\alpha D - \beta D^2),$$

where  $\alpha D$  accounts for the double-strand breaks induced by a single ionizing event, and the quadratic component  $\beta D^2$  accounts for the cell kill by multiple sublethal events.

The biological effective dose ( $\text{BED} = -1/\alpha \ln S$ ) represents the dose producing the same biological effect obtained under different irradiation conditions. The  $\alpha/\beta$  ratio relates the intrinsic radiosensitivity ( $\alpha$ ) and the potential sparing capacity ( $\beta$ ) for a specified tissue or effect.

In general, tissues with low  $\alpha/\beta$  values (normal tissues,  $\alpha/\beta = 2$ –5 Gy; kidneys,  $\alpha/\beta \sim 2.4$  Gy (46)) have more time to recover from sublethal damages and are more influenced by the dose rate compared with tissues with high  $\alpha/\beta$  values (tumor tissues,  $\alpha/\beta = 5$ –25 Gy).

On considering radionuclide therapy, the effect of the repair potential of the dose rate and of the delivery of the dose—protracted and possibly divided in cycles—must be included. Therefore, an additional parameter has been introduced in the LQ equation to finally provide a revised expression for the BED estimate (61,62):

$$\text{BED} = \sum_i D_i + \beta/\alpha \cdot T_{1/2\text{rep}}/(T_{1/2\text{rep}} + T_{1/2\text{eff}}) \cdot \sum_i D_i^2,$$

where  $D_i$  is the dose delivered per cycle  $i$ ,  $T_{1/2\text{rep}}$  is the repair half-time of sublethal damage, and  $T_{1/2\text{eff}}$  is the effective half-life of the radiopharmaceutical in the specific tissue.

This refined LQ model has been suggested with the intent of increasing the dose–response correlation in radionuclide therapy and applied, in particular, to PRRT, focusing on the kidney. Some results recently presented in the literature are briefly reported.

In a retrospective analysis on patients who received  $^{90}\text{Y}$ -DOTATOC therapy, dosimetry of the kidneys was reevaluated by the inclusion of some patient-specific adjustments. The contribution of this new approach was investigated for a possible dose–effect correlation for kidneys (50). In particular, according to the LQ model, the BED for kidneys was determined for each patient, considering the parameters derived from the specific biokinetics of  $^{90}\text{Y}$ -DOTATOC ( $T_{1/2\text{eff}} = 30$  h) and from the literature ( $T_{1/2\text{rep}} = 2.8$  h;  $\alpha/\beta = 2.6$  Gy) (54,62). The results of this study (50) strongly indicated that improvements in dosimetry reflect improved prediction of radiation effects. Accounting for the total activity administered in patients, the kidney absorbed dose range resulted in 19.4–39.6 Gy (when considering the actual kidney mass and the activity localized in the cortex), whereas the BED range was 27.7–59.3 Gy. Significantly, a correlation was found between BED and renal impairment (evaluated by means of loss of creatinine clearance per year), as opposed to the absorbed dose values alone, when evaluated by the standard or the refined methods as well. As a further relevant issue, it also emerged that patients with high BED and more serious kidney side effects received the treatment in a low number of cycles. These findings are consistent with other preliminary results reported in the literature (2,54,56), similarly suggesting an improved repair possibility for kidney tissues in the case of a higher number of cycles and a slow infusion of the radiocompounds over 1 h. Therefore, on the basis of the typical different sensitivities of most tumor tissues and kidney tissues to the dose rate and the number of cycles, treatment protocols based on multiple cycles could represent a powerful strategy to lower toxicity and, possibly, to improve the therapeutic outcome. Total administered activities could be increased accordingly.

## CONCLUSION

Patient variability requires careful individual dosimetry to determine the activity to be administered in PRRT. However, the value of the kidney absorbed dose may not be sufficient to accurately predict the likelihood of renal toxicity for individual patients. Other factors contribute to the biologic effectiveness, including the tissue radiosensitivity, dose rate, detailed intraorgan activity distribution, and cycle therapy scheme. New multiregional and radiobiologic models improve the prediction of dosimetry—in particular, the renal side effects. Moreover, the biologic equivalent dose approach strongly supports the need for

clinical randomized trials, which could definitively compare the therapeutic efficacy of equal therapeutic activities administered in multiple cycles versus a single or very few cycles.

## ACKNOWLEDGMENTS

The authors thank Prof. Giuliano Mariani and Dr. Marco Chinol for constructive discussion and Deborah Console for typing the manuscript. We are especially grateful to Prof. Mike Stabin and Prof. William Strauss for their support and valuable comments.

## REFERENCES

1. de Jong M, Kwekkeboom D, Valkema R, Krenning EP. Radiolabelled peptides for tumour therapy: current status and future directions—plenary lecture at the EANM 2002. *Eur J Nucl Med Mol Imaging*. 2003;30:463–469.
2. Bodei L, Cremonesi M, Grana C, et al. Receptor radionuclide therapy with  $^{90}\text{Y}$ -[DOTA]<sup>0</sup>-Tyr<sup>3</sup>-octreotide ( $^{90}\text{Y}$ -DOTATOC) in neuroendocrine tumours. *Eur J Nucl Med Mol Imaging*. 2004;31:1038–1046.
3. Valkema R, Pauwels SA, Kvoles LK, et al. Long-term follow-up of renal function after peptide receptor radiation therapy with  $^{90}\text{Y}$ -DOTA<sup>0</sup>-Tyr<sup>3</sup>-octreotide and  $^{177}\text{Lu}$ -DOTA<sup>0</sup>-Tyr<sup>3</sup>-octreotate. *J Nucl Med*. 2005;46(suppl 1):83S–91S.
4. Kwekkeboom DJ, Mueller-Brand J, Paganelli G, et al. An overview of the peptide receptor radionuclide therapy with 3 different radiolabeled somatostatin analogs. *J Nucl Med*. 2005;46(suppl 1):62S–66S.
5. Kwekkeboom DJ, Teunissen JJ, Bakker WH, et al. Radiolabeled somatostatin analog [ $^{177}\text{Lu}$ -DOTA<sup>0</sup>-Tyr<sup>3</sup>]octreotate in patients with endocrine gastroenteropancreatic tumors. *J Clin Oncol*. 2005;23:2754–2762.
6. Virgolini I, Britton K, Buscombe J, Moncayo R, Paganelli G, Riva P. In- and Y-DOTA-lanreotide: results and implications of the MAURITIUS trial. *Semin Nucl Med*. 2002;32:148–155.
7. Reubi JC, Mäcke HR, Krenning EP. Candidates for peptide receptor radiotherapy today and in the future. *J Nucl Med*. 2005;46(suppl 1):67S–75S.
8. Loevinger R, Budinger TF, Watson EE. *MIRD Primer*. Reston, VA: Society of Nuclear Medicine; 1999.
9. Siegel JA, Thomas SR, Stubbs JB, et al. Techniques for quantitative radiopharmaceutical biodistribution data acquisition and analysis for use in human radiation dose estimates: MIRD Pamphlet No.16. *J Nucl Med*. 1999;40(suppl):S37–S61.
10. Stabin M, Siegel J, Lipsztein J, et al. RADAR (RADiation Dose Assessment Resource). [www.doseinfo-radar.com](http://www.doseinfo-radar.com). Accessed July 18, 2006.
11. Stabin MG, Sparks RB, Crowe E. OLINDA/EXM: the second-generation personal computer software for internal dose assessment in nuclear medicine. *J Nucl Med*. 2005;46:1023–1027.
12. Ljungberg M, Frey E, Sjogreen K, Liu X, Dewaraja Y, Strand SE. 3D absorbed dose calculations based on SPECT: evaluation for  $^{111}\text{In}/^{90}\text{Y}$  therapy using Monte Carlo simulations. *Cancer Biother Radiopharm*. 2003;18:99–107.
13. Stabin MG, Kooij PP, Bakker WH, et al. Radiation dosimetry for indium-111-pentetreotide. *J Nucl Med*. 1997;38:1919–1922.
14. Kwekkeboom DJ, Kooij PP, Bakker WH, Macke HR, Krenning EP. Comparison of  $^{111}\text{In}$ -DOTA-Tyr<sup>3</sup>-octreotide and  $^{111}\text{In}$ -DTPA-octreotide in the same patients: biodistribution, kinetics, organ and tumor uptake. *J Nucl Med*. 1999;40:762–767.
15. Cremonesi M, Ferrari M, Zoboli S, et al. Biokinetics and dosimetry in patients administered with  $^{111}\text{In}$ -DOTA-Tyr<sup>3</sup>-octreotide: implications for internal radiotherapy with  $^{90}\text{Y}$ -DOTATOC. *Eur J Nucl Med*. 1999;26:877–886.
16. Forrer F, Uusijärvi H, Waldherr C, et al. A comparison of  $^{111}\text{In}$ -DOTATOC and  $^{111}\text{In}$ -DOTATATE: biodistribution and dosimetry in the same patients with metastatic neuroendocrine tumours. *Eur J Nucl Med Mol Imaging*. 2004;31:1257–1262.
17. Forrer F, Mueller-Brand J, Maecke H. Pre-therapeutic dosimetry with radiolabelled somatostatin analogues in patients with advanced neuroendocrine tumours. *Eur J Nucl Med Mol Imaging*. 2005;32:511–512.
18. Kwekkeboom DJ, Krenning EP, de Jong M. Peptide receptor imaging and therapy. *J Nucl Med*. 2000;41:1704–1713.
19. Valkema R, De Jong M, Bakker WH, et al. Phase I study of peptide receptor radionuclide therapy with [In-DTPA]octreotide: the Rotterdam experience. *Semin Nucl Med*. 2002;32:110–122.

20. Capello A, Krenning EP, Breeman WA, Bernard BF, de Jong M. Peptide receptor radionuclide therapy in vitro using [ $^{111}\text{In-DTPA}^0$ ]octreotide. *J Nucl Med.* 2003;44:98–104.
21. Waldherr C, Pless M, Maecke HR, et al. Tumor response and clinical benefit in neuroendocrine tumors after 7.4 GBq  $^{90}\text{Y-DOTATOC}$ . *J Nucl Med.* 2002;43:610–616.
22. Forster GJ, Engelbach MJ, Brockmann JJ, et al. Preliminary data on bio-distribution and dosimetry for therapy planning of somatostatin receptor positive tumours: comparison of  $^{86}\text{Y-DOTATOC}$  and  $^{111}\text{In-DTPA}$ -octreotide. *Eur J Nucl Med Mol Imaging.* 2001;28:1743–1750.
23. Helisch A, Förster GJ, Reber H, et al. Pre-therapeutic dosimetry and biodistribution of  $^{86}\text{Y-DOTA-Phe 1-Tyr 3-octreotide}$  versus  $^{111}\text{In-pentetreotide}$  in patients with advanced neuroendocrine tumours. *Eur J Nucl Med Mol Imaging.* 2004;31:1386–1392.
24. Pauwels S, Barone R, Walrand S, et al. Practical dosimetry of peptide receptor radionuclide therapy with  $^{90}\text{Y}$ -labeled somatostatin analogs. *J Nucl Med.* 2005;46(suppl 1):92S–98S.
25. de Jong M, Bakker WH, Breeman WA, et al. Pre-clinical comparison of [DTPA $^0$ ] octreotide, [DTPA $^0$ ,Tyr $^3$ ] octreotide and [DOTA $^0$ ,Tyr $^3$ ] octreotide as carriers for somatostatin receptor-targeted scintigraphy and radionuclide therapy. *Int J Cancer.* 1998;75:406–411.
26. Pentlow KS, Finn RD, Larson SM, Erdi YE, Beattie BJ, Humm JL. Quantitative imaging of yttrium-86 with PET: the occurrence and correction of anomalous apparent activity in high density regions. *Clin Positron Imaging.* 2000;3:85–90.
27. Walrand S, Jamar F, Mathieu I, et al. Quantitation in PET using isotopes emitting prompt single gammas: application to yttrium-86. *Eur J Nucl Med Mol Imaging.* 2003;30:354–361.
28. Buchholz HG, Herzog H, Forster GJ, et al. PET imaging with yttrium-86: comparison of phantom measurements acquired with different PET scanners before and after applying background subtraction. *Eur J Nucl Med Mol Imaging.* 2003;30:716–720.
29. Walrand S, Barone R, Jamar F, et al. Red marrow  $^{90}\text{Y-OctreoTher}$  dosimetry estimated using  $^{86}\text{Y-OctreoTher}$  PET and biological correlates [abstract]. *Eur J Nucl Med Mol Imaging.* 2002;29(suppl):434.
30. Kwekkeboom DJ, Bakker WH, Kooij PP, et al. [ $^{177}\text{Lu-DOTAOTyr}^3$ ]octreotate: comparison with [ $^{111}\text{In-DTPA}^0$ ]octreotide in patients. *Eur J Nucl Med.* 2001;28:1319–1325.
31. de Jong M, Breeman WA, Valkema R, Bernard BF, Krenning EP. Combination radionuclide therapy using  $^{177}\text{Lu}$ - and  $^{90}\text{Y}$ -labeled somatostatin analogs. *J Nucl Med.* 2005;46(suppl 1):13S–17S.
32. Stabin MG, Eckerman KF, Bolch WE, Bouchet LG, Patton PW. Evolution and status of bone and marrow dose models. *Cancer Biother Radiopharm.* 2002;17:427–433.
33. Sgouros G. Dosimetry of internal emitters. *J Nucl Med.* 2005;46(suppl 1):18S–27S.
34. Stabin MG, Siegel JA, Sparks RB. Sensitivity of model-based calculations of red marrow dosimetry to changes in patient-specific parameters. *Cancer Biother Radiopharm.* 2002;17:535–543.
35. Sgouros G. Bone marrow dosimetry for radioimmunotherapy: theoretical considerations. *J Nucl Med.* 1993;34:689–694.
36. Behr TM, Behe M, Sgouros G. Correlation of red marrow radiation dosimetry with myelotoxicity: empirical factors influencing the radiation-induced myelotoxicity of radiolabeled antibodies, fragments and peptides in pre-clinical and clinical settings. *Cancer Biother Radiopharm.* 2002;17:445–464.
37. Forssell-Aronsson E, Fjalling M, Nilsson O, Tisel LE, Wangberg B, Ahlman H. Indium-111 activity concentration in tissue samples after intravenous injection of indium-111-DTPA-D-Phe-1-octreotide. *J Nucl Med.* 1995;36:7–12.
38. Maecke HR, Hofmann M, Haberkorn U.  $^{68}\text{Ga}$ -Labeled peptides in tumor imaging. *J Nucl Med.* 2005;46(suppl 1):172S–178S.
39. Henze M, Dimitrakopoulou-Strauss A, Milker-Zabel S, et al. Characterization of  $^{68}\text{Ga-DOTA-D-Phe1-Tyr3-octreotide}$  kinetics in patients with meningiomas. *J Nucl Med.* 2005;46:763–769.
40. Wester HJ, Schottelius M, Scheidhauer K, et al. PET imaging of somatostatin receptors: design, synthesis and preclinical evaluation of a novel  $^{18}\text{F}$ -labelled, carboxylated analogue of octreotide. *Eur J Nucl Med Mol Imaging.* 2003;30:117–122.
41. Chen X, Park R, Hou Y, et al. MicroPET and autoradiographic imaging of GRP receptor expression with  $^{64}\text{Cu-DOTA-[Lys}^3\text{]bombesin}$  in human prostate adenocarcinoma xenografts. *J Nucl Med.* 2004;45:1390–1397.
42. Rogers BE, Manna DD, Safavy A. In vitro and in vivo evaluation of a  $^{64}\text{Cu}$ -labeled polyethylene glycol-bombesin conjugate. *Cancer Biother Radiopharm.* 2004;19:25–34.
43. Anderson CJ, Dehdashti F, Cutler PD, et al.  $^{64}\text{Cu-TETA}$ -octreotide as a PET imaging agent for patients with neuroendocrine tumors. *J Nucl Med.* 2001;42:213–221.
44. Lambert B, Cybulla M, Weiner SM, et al. Renal toxicity after radionuclide therapy. *Radiat Res.* 2004;161:607–611.
45. Breitz HB, Wendt RE 3rd, Stabin MS, et al.  $^{166}\text{Ho-DOTMP}$  radiation-absorbed dose estimation for skeletal targeted radiotherapy. *J Nucl Med.* 2006;47:534–542.
46. de Jong M, Valkema R, Van Gameren A, et al. Inhomogeneous localization of radioactivity in the human kidney after injection of [ $^{111}\text{In-DTPA}$ ]octreotide. *J Nucl Med.* 2004;45:1168–1171.
47. Bouchet LG, Bolch WE, Blanco HP, et al. MIRDO Pamphlet No. 19: absorbed fractions and radionuclide S values for six age-dependent multiregion models of the kidney. *J Nucl Med.* 2003;44:1113–1147.
48. Green A, Flynn A, Pedley RB, Dearing J, Begent R. Nonuniform absorbed dose distribution in the kidney: the influence of organ architecture. *Cancer Biother Radiopharm.* 2004;19:371–377.
49. Konijnenberg MW, De Jong M, Valkema R, Krenning EP. Combined functional status and dose-volume analysis for determining renal damage threshold with radionuclide therapy [abstract]. *Eur J Nucl Med Mol Imaging.* 2004;31:S239.
50. Barone R, Borson-Chazot F, Valkema R, et al. Patient-specific dosimetry in predicting renal toxicity with  $^{90}\text{Y-DOTATOC}$ : relevance of kidney volume and dose rate in finding a dose–effect relationship. *J Nucl Med.* 2005;46(suppl 1):99S–106S.
51. Rolleman EJ, Valkema R, de Jong M, Kooij PP, Krenning EP. Safe and effective inhibition of renal uptake of radiolabelled octreotide by a combination of lysine and arginine. *Eur J Nucl Med Mol Imaging.* 2003;30:9–15.
52. Behr TM, Goldenberg DM, Becker W. Reducing the renal uptake of radiolabeled antibody fragments and peptides for diagnosis and therapy: present status, future prospects and limitations. *Eur J Nucl Med.* 1998;25:201–212.
53. Bernard BF, Krenning EP, Breeman WA, et al. D-Lysine reduction of indium-111 octreotide and yttrium-90 octreotide renal uptake. *J Nucl Med.* 1997;38:1929–1933.
54. Barone R, De Camps J, Smith C, et al. Amino acid (AA) solutions infused for renal radioprotection: metabolic effects [abstract]. *Nucl Med Commun.* 2000;21:563.
55. Cremonesi M, Bodei L, Rocca P, Stabin M, Macke HR, Paganelli G. Kidney protection during receptor-mediated radiotherapy  $^{90}\text{Y-DOTA}^0\text{-Tyr}^3\text{-octreotide}$  [abstract]. *Cancer Biother Radiopharm.* 2002;17:344.
56. Bodei L, Cremonesi M, Zoboli S, et al. Receptor-mediated radionuclide therapy with  $^{90}\text{Y-DOTATOC}$  in association with amino acid infusion: a phase I study. *Eur J Nucl Med Mol Imaging.* 2003;30:207–216.
57. Jamar F, Barone R, Mathieu I, et al.  $^{86}\text{Y-DOTA}^0\text{-d-Phe}^1\text{-Tyr}^3\text{-octreotide}$  (SMT487): a phase I clinical study—pharmacokinetics, biodistribution and renal protective effect of different regimens of amino acid co-infusion. *Eur J Nucl Med Mol Imaging.* 2003;30:510–518.
58. Emami B, Lyman J, Brown A, et al. Tolerance of normal tissue to therapeutic irradiation. *Int J Radiat Oncol Biol Phys.* 1991;21:109–122.
59. Kassis AI, Adelstein SJ. Radiobiologic principles in radionuclide therapy. *J Nucl Med.* 2005;46(suppl 1):4S–12S.
60. O'Donoghue J. Relevance of external beam dose-response relationships to kidney toxicity associated with radionuclide therapy. *Cancer Biother Radiopharm.* 2004;19:378–387.
61. Dale R. Use of the linear-quadratic radiobiological model for quantifying kidney response in targeted radiotherapy. *Cancer Biother Radiopharm.* 2004;19:363–370.
62. Konijnenberg MW. Is the renal dosimetry for [ $^{90}\text{Y-DOTA}^0\text{-Tyr}^3$ ]octreotide accurate enough to predict thresholds for individual patients? *Cancer Biother Radiopharm.* 2003;18:619–625.